Journal of Alloys and Compounds 520 (2012) 114–121

Contents lists available at SciVerse ScienceDirect

Journal of Alloys and Compounds

journal homepage: www.elsevier.com/locate/jallcom

Preparation and microwave absorbing properties of nickel-coated graphite nanosheet with pyrrole via in situ polymerization

Yongqing Yang [a,*], Shuhua Qi [a], Jianning Wang [b]

[a] Department of Applied Chemistry, School of Science, Northwestern Polytechnical University, Xi'an 710072, China
[b] Personnel Department, Ningxia University, Yinchuan 710052, China

ARTICLE INFO

Article history:
Received 8 August 2011
Received in revised form
28 December 2011
Accepted 28 December 2011
Available online 3 January 2012

Keywords:
In situ polymerization
Nanostructured materials
Microwave absorbing property
Conductive polymer
Microstructure

ABSTRACT

Nanocomposites PPy/NanoG and PPy/Ni/NanoG were prepared via in situ polymerization of pyrrole in the presence of NanoG and nickel-coated graphite nanosheet (Ni/NanoG), respectively. The morphologies and nanostructures of NanoG, Ni/NanoG, PPy, PPy/NanoG and PPy/Ni/NanoG were characterized by scanning electron microscope (SEM), energy dispersive spectroscopy (EDS), Fourier transmission infrared (FTIR) and X-ray diffraction analysis (XRD). Results show that most of PPy chains disperse on NanoG and Ni/NanoG's surfaces for the high aspect ratio (300–500) of NanoG and Ni/NanoG. From the thermogravimetric analysis (TG) it can be seen that the introduction of Ni and NanoG leads the composites PPy/NanoG and PPy/Ni/NanoG to exhibit a better thermal stability than pure PPy. According to the four-point-probe test, the conductivities of the final PPy/NanoG and PPy/Ni/NanoG composites are dramatically increased compared to pure PPy. Measurement of electromagnetic parameters shows that the reflection loss (R) of PPy/Ni/NanoG is below −19 dB at the X band (8.2–12.4 GHz) and the minimum loss value is −23.46 dB at 9.88 GHz. The reflection loss of PPy/NanoG is below −10 dB at 8.2–12.4 GHz and the minimum loss value is −13.44 dB at 10.28 GHz. The microwave absorbing properties of PPy/NanoG and PPy/Ni/NanoG are superior to those of PPy.

1. Introduction

With the development of modern informationized warfare, microwave absorbing materials have absorbed much attention [1,2]. To get the microwave absorbing materials with combination properties as thin in thickness, light in weight, broad in frequency and strong in absorbing peak, much work has been done.

According to the absorbing mechanism, microwave absorbing materials can be divided into two types: magnetic materials and electronic materials. The absorbing properties of the microwave absorbing materials can be expressed by the following parameters [3,4]: complex permittivity ($\varepsilon^* = \varepsilon' - j\varepsilon''$), complex permeability ($\mu^* = \mu' - j\mu''$), dielectric loss ($\tan\delta_e = \varepsilon''/\varepsilon'$) and magnetic loss ($\tan\delta_m = \mu''/\mu'$). The higher the imaginary parts of the complex permittivity (ε'') and the complex permeability (μ'') as well as the higher $\tan\delta_e$ and $\tan\delta_m$, the higher absorbing properties of the materials are.

Recently, inherently conducting polymers such as polyacetylene (PA), polypyrrole (PPy), polyaniline (PANI) and polythiophene (PTH) are deeply investigated for their good conductivity and light in weight [5–8]. Up to the present, several groups have done much work on synthesizing electromagnetic PPy-based nanocomposites [9–11]. Conductive materials such as carbon black [12], carbon fiber [13], carbon nano-tube [14], magnetic materials [15–17] such as ferrite, crystal whisker and nano-metals are always added into them. Among them, conductive material graphite has absorbed much attention for its unique mechanical, chemical and electrical properties. Graphite is well known to be as a layered material with high conductivity, which can be intercalated by chemical reagents such as nitric acid (HNO_3) or sulfuric acid (H_2SO_4) and form into another kind of compound called graphite intercalation compounds (GIC). By rapid thermal treatment, GIC can expand several hundreds times the volume of its original and get expanded graphite (EG) [18–20].

In this paper, NanoG with high conductivity was prepared by ultrasonication of EG in an aqueous ethanol solution. To further improve the magnetic properties of the composites and enlarge their application, some metals are always chemically coated on NanoG's surface. Among the metals, Ni was chosen for its high magnetic properties, low price and stability. The aim of this work was to fabricate the nanocomposites via in situ polymerization of pyrrole in the presence of NanoG and Ni/NanoG. The morphologies and nanostructures of NanoG, Ni/NanoG, PPy, PPy/NanoG and PPy/Ni/NanoG were characterized by SEM, EDS, FTIR and XRD. Properties such as thermal stability, conductivity and microwave absorbing of them were measured.

* Corresponding author.
E-mail address: ylqqyyq@yahoo.cn (Y. Yang).

0925-8388/$ – see front matter © 2012 Published by Elsevier B.V.
doi:10.1016/j.jallcom.2011.12.136

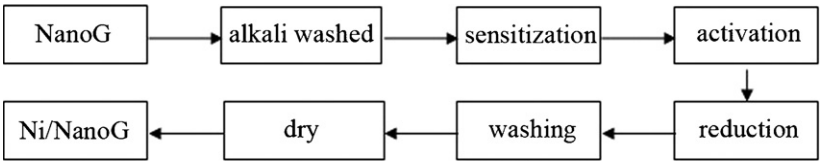

Fig. 1. Preparation of Ni/NanoG.

2. Experimental

2.1. Materials

The oxidized graphite (OG) was supplied by Shandong Qingdao Graphite Company (Qingdao, China). Pyrrole (Py, AR) was bought from Sinopharm Chemical Reagent Limited Company and was distilled in reduced pressure before being used. Ferric chloride ($FeCl_3{\cdot}6H_2O$), palladium chloride ($PdCl_2$) and tin chloride dehydrate ($SnCl_2{\cdot}2H_2O$) were bought from Chemical Company of Tianjin. Sodium hypophosphite (NaH_2PO_2), nickel sulfate ($NiSO_4{\cdot}6H_2O$), 36% hydrochloric acid (HCl), sodium hydroxide (NaOH), ammonia ($NH_3{\cdot}H_2O$), 3-triethoxysilyl-propylamine (KH550) and ethanol of analytical reagent grade were purchased from Chemical Company of Xi'an.

2.2. Synthesis of NanoG

NanoG was prepared from the oxidized graphite (OG) by two steps. OG was firstly subjected to a thermal expansion at 900–1000 °C for 15 s in a muffe furnace to form EG. Then EG was immersed in an aqueous solution containing 70% ethanol and 30% distilled water and exfoliated in an ultrasonic bath for 24 h. The product was then filtered, washed and dried in a vacuum at 80 °C for about 8 h to get NanoG. The preparation processes of NanoG are as follows:

$$\text{Oxidized graphite (OG)} \xrightarrow{900-1000\,^{\circ}\text{C},\ 15\,\text{s}} \text{Expanded graphite (EG)} \xrightarrow{\text{ultrasonic}} \text{NanoG} \quad (1)$$

2.3. Synthesis of Ni/NanoG

The preparation of Ni/NanoG involve an initial pretreatment of NanoG and a subsequent reduction of $NiSO_4$ in the presence of NaH_2PO_2. The process is shown as Fig. 1.

NanoG was firstly alkali washed in the 10% NaOH solution for about an hour to get rid of the impurity and then sensitized by 1% $SnCl_2{\cdot}2H_2O$ for about 0.5 h. After that, the sensitized NanoG was activated by $PdCl_2$ to enhance the adhesion force between the silver coating and NanoG. The reaction of $SnCl_2{\cdot}2H_2O$ and $PdCl_2$ is as follows:

$$Sn^{2+} + Pd^{2+} = Sn^{4+} + Pd \quad (2)$$

The mechanism of the reaction is as follows:

$$SnCl_2 + H_2O \rightarrow Sn(OH)Cl + H^+ + Cl^- \quad (3)$$

$$SnCl_2 + 2H_2O \rightarrow Sn(OH)_2 + 2H^+ + 2Cl^- \quad (4)$$

$$Sn(OH)Cl + Sn(OH)_2 \rightarrow Sn_2(OH)_3Cl \quad (5)$$

$$Sn_2(OH)_3Cl + 2PdCl_2 \rightarrow Sn_2(OH)_3Cl_5 + 2Pd \quad (6)$$

The obtained Pd was used as catalyst in the following procedure.

After these steps, NanoG was dispersed by ultrasonic wave for 30 min and then discharged into a flask with a mixture of nickel sulfate, ammonia, malic acid and distilled water. The mixture was stirred at 70 °C for 30 min and the pH was kept at 8–9. Then the reducing agent (10% NaH_2PO_2) was added into the flask dropwise. The reaction was carried out at 70 ± 2 °C for about 1 h. After the reaction, 1 mol/L NaOH was used to adjust pH to be in the range of 10.5–11. Then the suspension was filtered, washed several times with distilled water and dried in an oven at about 50 °C. The reaction is as follows:

$$Ni^{2+} + 4H_2PO_2^- + H_2O = Ni + P + 3HPO_3^{2-} + 4H^+ + (3/2)H_2 \quad (7)$$

2.4. Synthesis of PPy/NanoG and PPy/Ni/NanoG nanocomposites

PPy/NanoG was prepared via in situ polymerization. An amount of NanoG was firstly added into the 3-triethoxysilylpropylamine (KH550) solution and dispersed by ultrasonication for about an hour. After filtrated and washed by distilled water, the pretreated NanoG and a mixture of ethanol, distilled water, 1 M HCl solution were discharged into a flask with string. The mixture was sonicated for 1 h. Then pyrrole was added into the flask. After the temperature of the mixture fell below 5 °C, a solution of $FeCl_3{\cdot}6H_2O$ was dropped into the mixture and the reaction was carried out for 6 h. The color of the mixture changed from yellow green to dark green.

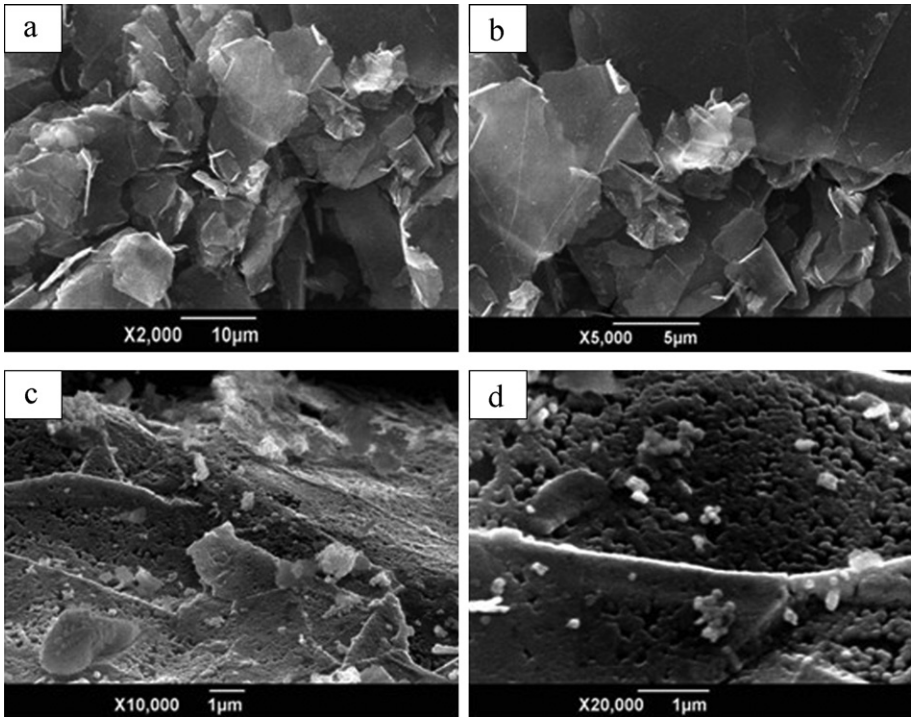

Fig. 2. SEM images of NanoG and Ni/NanoG.

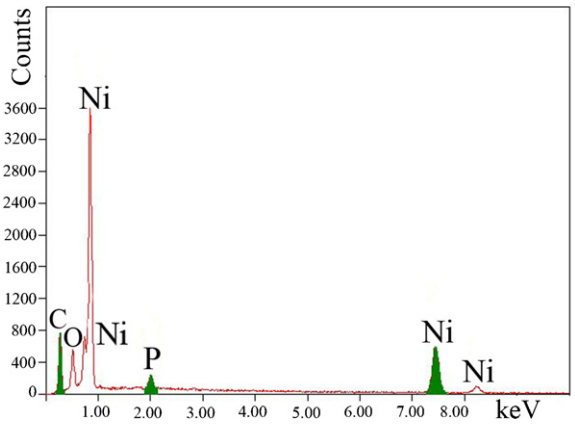

Fig. 3. EDS of Ni/NanoG.

The resulting precipitate was filtrated, washed with distilled water and ethanol repeatedly and dried under vacuum at 60 °C for about 24 h.

PPy/Ni/NanoG nanocomposite was synthesized by in situ polymerization as above.

2.5. Characterization

The structures of NanoG, Ni/NanoG, PPy, PPy/NanoG and PPy/Ni/NanoG were characterized by using scanning electron microscope (SEM; JSM-6390, HITACHI, Japan), energy dispersive spectroscopy analyzer (EDS: JED-2200 Series), WQF-510 FTIR spectrometer (Ruili, China) and X-ray diffractogramms (XRD; PANalytical, Holland), respectively.

The electrical conductivities of NanoG, Ni, Ni/NanoG, PPy, PPy/NanoG and PPy/Ni/NanoG nanocomposites were measured by using a SZ-82 digital four probes resistance tester (Suzhou Electronic Equipment Factory, China). For measurement of electrical properties, circle samples with a diameter of 15 mm and a thickness of 2 mm were prepared by casting them into the stainless forms and cold-pressed. The thermal stabilities of PPy, PPy/NanoG and PPy/Ni/NanoG nanocomposites were analyzed by using a thermogravimetric analysis (TG, SDT-2960, USA) with a heating rate of 10 °C/min in the range from 20 to 800 °C under nitrogen atmosphere. The electormagnetic parameters of them were analyzed by using a HP8753D vector network analyzer and the samples were made as 22.86 mm × 10.16 mm × 2 mm.

3. Results and discussion

3.1. SEM and EDS analysis

3.1.1. SEM images of NanoG and Ni/NanoG

NanoG was prepared by treating EG with ultrasonication in an aqueous solution of 70% ethanol and 30% distilled water. Fig. 2(a and b) shows the SEM images of NanoG. It can be seen that EG has been efficiently exfoliated to ultra thin transparent graphite nanosheets with a width about 1–20 μm and a thickness about 30–90 nm, indicating a large aspect ratio (300–500) of NanoG. The higher the aspect ratio of the material, the lower the filler content as well as the higher electrical conductivity.

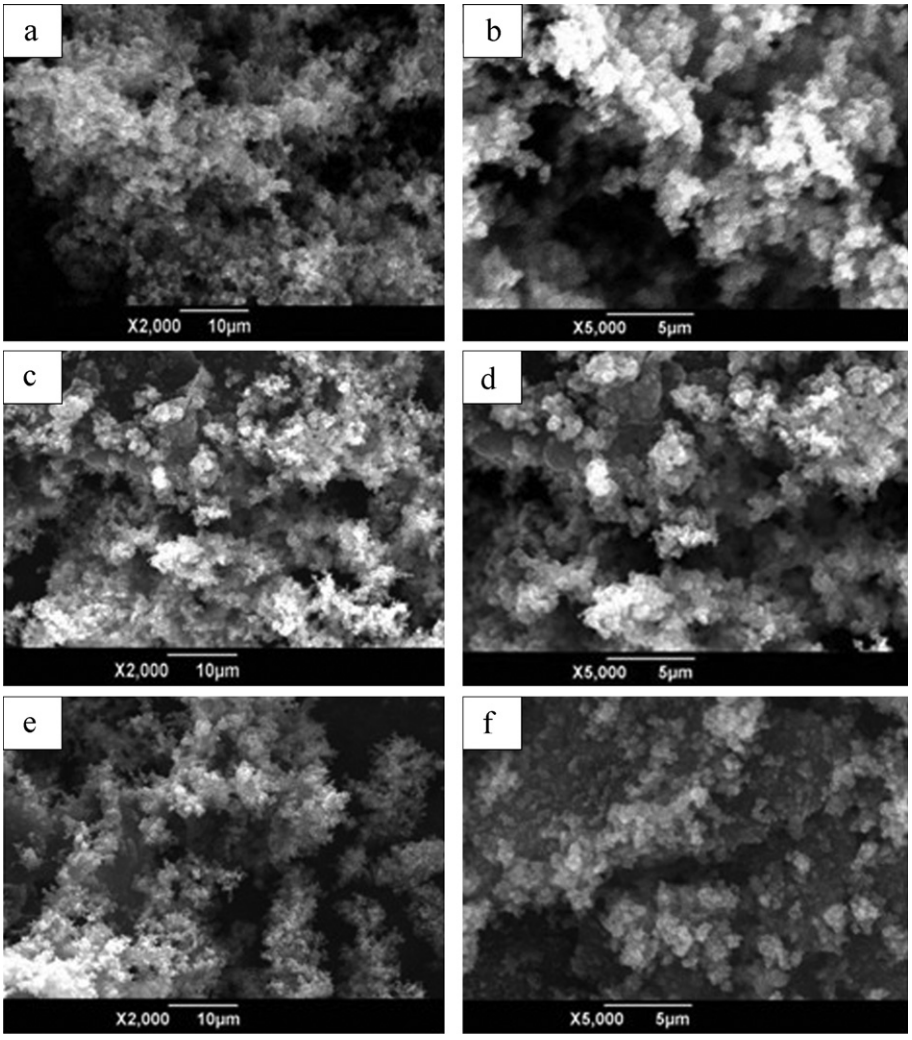

Fig. 4. SEM images of PPy (a and b), PPy/NanoG (c and d) and PPy/Ni/NanoG (e and f).

Table 1
Elements analysis of Ni/NanoG.

Element	keV	mass%	atom %
C K	0.277	28.67	63.88
O K	0.525	1.51	3.38
P K	2.013	2.25	1.94
Ni K	7.471	67.57	30.80
Total		100.00	100.00

Ni/NanoG was prepared by chemical reaction between oxidant $NiSO_4$ and reductant NaH_2PO_2 on NanoG's surface. The SEM images of Ni/NanoG with a magnification of 10,000 and 20,000 are shown in Fig. 2(c and d). It can be seen that NanoG's surface is tightly covered by Ni nanoparticles. The thickness of Ni/NanoG is about 200–250 nm.

3.1.2. EDS of Ni/NanoG

Elements and their quantities of Ni/NanoG were measured by EDS analysis. Fig. 3 confirms the presence of C, Ni, P and O in the Ni/NanoG. The mass content of Ni in Ni/NanoG reaches 67.57% (seen in Table 1), which can further reflect the covering of C by Ni. The little element O may come from the functional group of —OH and —COOH on the graphite nanosheets. The mass content of P is 2.25%, indicating the low P content in the coating. The lower the P content, the higher the conductivity of the coating.

3.1.3. SEM images of PPy, PPy/NanoG and PPy/Ni/NanoG

PPy was prepared by in situ polymerization and the structure of it could be clearly characterized by SEM images. Fig. 4(a and b) suggests that PPy appear to be spherical shape and connect with each other. The diameter of them can reach nanometer grade. Fig. 4(c, d) and (e, f) demonstrate the surface morphologies of PPy/NanoG and PPy/Ni/NanoG, respectively. It can be seen that there are lots of small bright nanoparticles on NanoG and Ni/NanoG's surfaces. During the in situ polymerization, NanoG and Ni/NanoG are firstly pretreated by KH550. After hydrolysis, KH550 can produce methylsilane functional groups, which can connect NanoG with PPy. At the same time, NanoG and Ni/NanoG are used as hard templates. Pyrrole can easily react on their surfaces and hydrogen bond can form between —H provided by PPy and —OH provided by NanoG and Ni/NanoG. The flake-like structure of NanoG and Ni/NanoG can restrain PPy chains from tangling with each other. So the dispersities of the composites PPy/NanoG and PPy/Ni/NanoG are improved compared to those of PPy.

3.2. XRD analysis

The crystal structure of NanoG and Ni/NanoG were characterized by XRD analysis and the recorded diffractograms were shown in Fig. 5 (1 and 2). The peaks at $2\theta = 26.46^\circ$ and 55.64° are corresponding to (0 0 2) and (1 1 0) planes respectively and are the typical diffraction peaks of graphite (JCPDS. File No. 75-1621). In Fig. 5(2b), another three diffraction peaks at 44.52°, 51.84° and 76.39° can be observed, which indicate the (1 1 1), (2 0 0) and (2 2 0) planes of nickel's cubic face-centered structure (JCPDS. No. 04-0805). In Fig. 5(2c), that is, the X-ray diffractogram curve of Ni/NanoG, the typical planes of both graphite (0 0 2), (1 1 1) and nickel (1 1 1), (2 0 0), (2 2 0) can be seen, which agree well with earlier reports [21–24]. The diffraction peaks of Ni/NanoG are relatively weaker than those of NanoG and Ni, respectively. It indicates that NanoG's

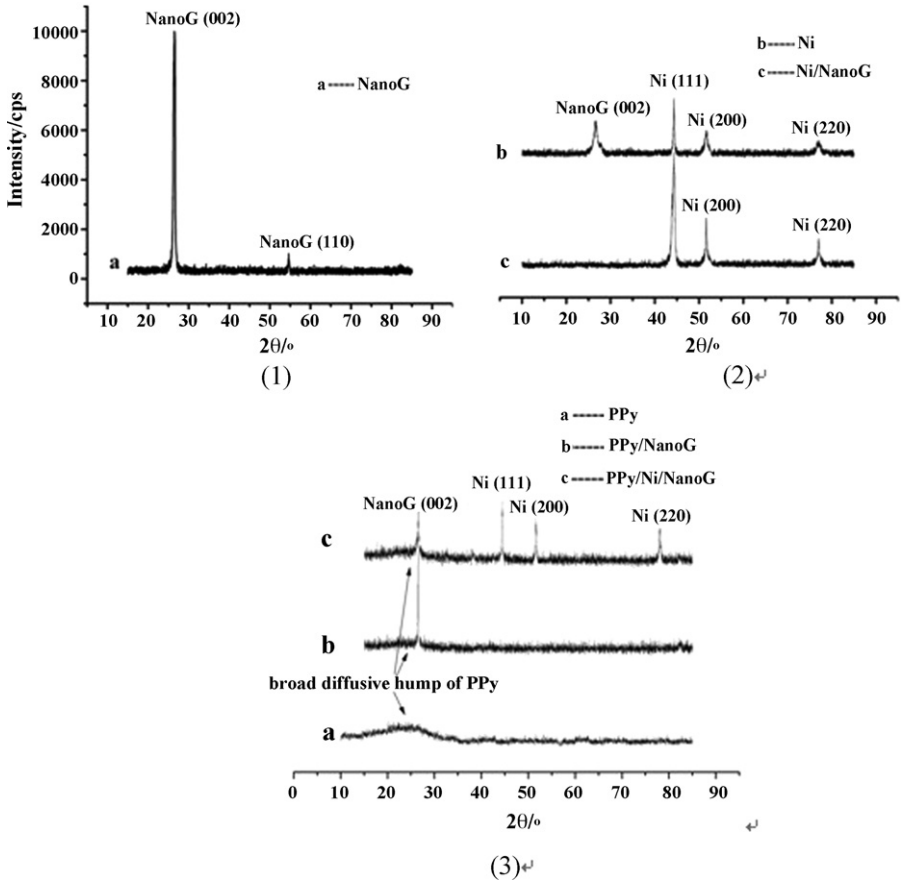

Fig. 5. X-ray diffraction curves of NanoG (1a), Ni (2b), Ni/NanoG (2c), PPy (3a), PPy/NanoG (3b) and PPy/Ni/NanoG (3c).

Table 2
FTIR absorption peaks of PPy, PPy/NanoG and PPy/Ni/NanoG.

Wave numbers (cm^{-1})			Functional group affiliation
PPy	PPy/NanoG	PPy/Ni/NanoG	
3427	3438	3434	N—H stretching vibrations
1620	1633	1637	N—H in-plane deformation vibrations
1524	1554	1548	C—C stretching vibrations
1424	1442	1477	C—N stretching vibrations
1155	1160	1191	=C—H in-plane deformation vibrations
1022	1035	1045	N—H out-of-plane deformation vibrations
885	887	927	=C—H out-of-plane deformation vibrations
659	677	686	C—C out-of-plane deformation vibrations

surface is covered by nickel particles which weaken the diffraction peak's strength of NanoG.

The structures of PPy, PPy/NanoG and PPy/Ni/NanoG were characterized by XRD analysis. The results are shown in Fig. 5(3). Fig. 5(3a) shows that there is a broad diffusive hump at $2\theta = 15–30^{\circ}$, indicating the amorphous nature of PPy. As known to us all, most of α—α′ bonds are formed during the in situ polymerization of pyrrole by chemical oxidization. At the same time, some α—β bonds can also be formed which damage the sequential of the polymer chains and lead to the amorphous nature of the polymer. Fig. 5(3b) shows the X-ray diffractogram pattern of PPy/NanoG. The peak at 26.46° is the typical (0 0 2) plane of graphite. A relatively weaker broad peak can also be seen at $2\theta = 15–30^{\circ}$. Fig. 5(3c) demonstrates the X-ray diffractogram pattern of PPy/Ni/NanoG. The typical planes of both graphite (0 0 2) and nickel (1 1 1), (2 0 0), (2 2 0) can be seen. The relative intensities of all diffraction peaks in PPy/NanoG and PPy/Ni/NanoG are weaker than those of PPy. The addition of NanoG and Ni/NanoG can have a great effect on the PPy such as the degree of its being doped, the force among the PPy chains, thus affect the strength of the diffraction peaks.

3.3. FTIR analysis of PPy, PPy/NanoG and PPy/Ni/NanoG

The functional groups of PPy, PPy/NanoG and PPy/Ni/NanoG are measured by FTIR analysis. Results are shown in Fig. 6. All the three investigated samples have the typical absorbing peaks of PPy as shown in Fig. 6(a). The band at 3427 cm^{-1} corresponds to the N—H stretching vibrations of pyrrole ring. The band at 1620 cm^{-1} relates to the N—H in-plane deformation vibrations and 1424 cm^{-1} reflects to the C—N stretching vibrations. The =C—H in-plane deformation vibrations is situated at 1155 cm^{-1} and the C—C stretching vibrations can be seen at 1524 cm^{-1}. The out-of-plane deformation vibrations of the N—H and C—H are situated at 1022 cm^{-1} and 885 cm^{-1}. The above results indicate the formation of PPy by in situ polymerization.

Fig. 6(b) and (c) is the FTIR spectra of PPy/NanoG and PPy/Ni/NanoG. The wave numbers of the composites PPy/NanoG and PPy/Ni/NanoG are shown in Table 2. The typical absorbing peaks of PPy can also be seen in FTIR spectra of PPy/NanoG and PPy/Ni/NanoG. From the data in Table 2, it can be seen that compare to PPy FTIR spectrum, all the absorption peaks of PPy/NanoG and PPy/Ni/NanoG have great blue shifts, that is the peaks shift from the lower wave numbers to the higher wave numbers. It indicates that the vibration and the degree of the electron delocalization of PPy chain have great changes after compounding with NanoG and Ni/NanoG. All these are attributed to the small particles size effect and quantum size effect of NanoG and Ni/NanoG.

3.4. TG analysis

In this paper, NanoG and Ni/NanoG are used as hard templates and conductive fillers to improve the properties of PPy. Fig. 7 shows the TG curves of PPy (a), PPy/NanoG (b) and PPy/Ni/NanoG (c) nanocomposites, respectively. It can be seen that all the curves show only one decomposition peak. The weight loss about of 10% in the temperature range from 0 to 100 °C comes from the volatilization of the water. The degradation temperatures of PPy, PPy/NanoG and PPy/Ni/NanoG are all about 300 °C for the pyrolysis of the main-chain. PPy has residue of 21.80 wt% at 750 °C while PPy/NanoG and PPy/Ni/NanoG nanocomposites have residues about 30.37 wt% and 46.28 wt%, respectively. Temperatures corresponding to the different weight loss such as 20%, 25%, 30%, 35% are shown in Table 3. Data indicate that all the corresponding temperatures in the PPy/NanoG and PPy/Ni/NanoG curves are higher than those in the PPy curve. These finding can result from the role of NanoG in imposing restriction on the pyrolysis of PPy chains and avoid heat concentration,

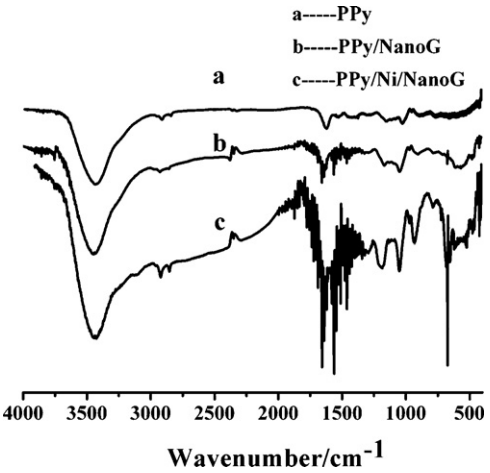

Fig. 6. FTIR spectra of PPy (a), PPy/NanoG (b) and PPy/Ni/NanoG (c).

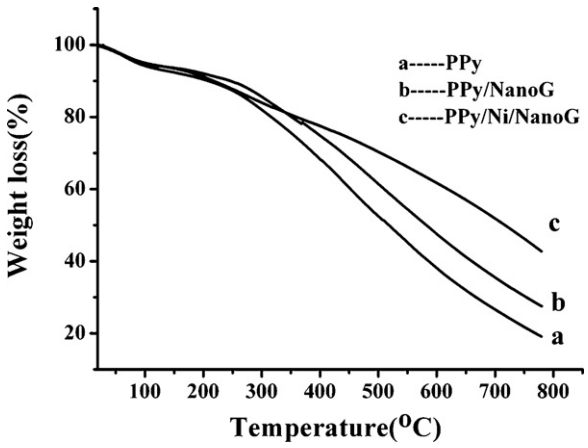

Fig. 7. TG curves of PPy (a), PPy/NanoG (b) and PPy/Ni/NanoG (c).

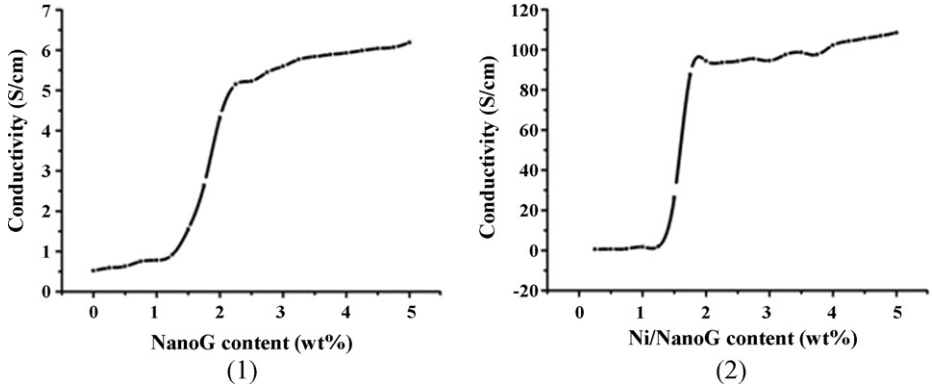

Fig. 8. Conductivities of PPy/NanoG and PPy/Ni/NanoG with different NanoG and Ni/NanoG contents.

Table 3
The different temperature at different weight loss (20%, 25%, 30%, 35%).

Samples	Weight loss (wt%)			
	20	25	30	35
Pure PPy	316.32	354.99	389.29	422.32
PPy/NanoG	351.10	398.84	438.90	475.27
PPy/Ni/NanoG	359.79	438.59	504.01	563.14

Table 4
Conductivity values of NanoG, Ni and Ni/NanoG (S/cm).

Sample	NanoG	Ni	Ni/NanoG
Conductivity	9.06×10^3	9.56×10^4	6.67×10^4

Table 5
Conductivity values of PPy, PPy/NanoG and PPy/Ni/NanoG (S/cm).

Samples	PPy	PPy/NanoG	PPy/Ni/NanoG
Conductivity values	0.52	5.15	87.58

which suggest that there is a strong interaction among the nickel particles, NanoG and PPy chains.

3.5. Electrical analysis

The electrical conductivities of NanoG, Ni, Ni/NanoG, PPy, PPy/NanoG and PPy/Ni/NanoG were measured by using a SZ-82 digital four probes resistance tester. Results are shown in Tables 4–6. The conductivity of NanoG can reach 9.06×10^3 S/cm, indicates that NanoG is a good conductor, while the conductivity of Ni can reach 9.56×10^4 S/cm. After assembling NanoG and Ni together, the conductivity of Ni/NanoG is 6.67×10^4 S/cm, which is higher than NanoG but lower than Ni. Wrapped up by Ni, the conductivity of NanoG can enhance prominently.

Conductivities of PPy/NanoG and PPy/Ni/NanoG with different NanoG and Ni/NanoG contents are shown in Fig. 8. Fig. 8(1) depicts the change of electrical conductivity as a function of NanoG content. The conductivities of PPy/NanoG are dramatically increased with the increasing of NanoG contents. When the mass ratio of NanoG to PPy is 2.25%, the conductivity of PPy/NanoG reaches 5.15 S/cm. After that, with the increase of NanoG content, the electrical conductivity still increases with a small extent. The reason is that NanoG is well-proportioned dispersed in the composite and the conductive network cannot be formed when the quantity of NanoG is low. In this circumstance, the conductivity of the composite is primarily from PPy. With the higher contents of NanoG, the particles of it connect with each other and some conductive networks can form which contribute to the conductivity of the composite. When the NanoG content reaches a critical value, the networks contact with each other and the conductive passageways are formed, leading to higher conductivity.

Table 6
Percolation thresholds of NanoG and Ni/NanoG used in the composites (wt%).

Fillers	NanoG	Ni/NanoG
Percolation	2.25	1.75

As to PPy/Ni/NanoG, the conductivity value of it with a Ni/NanoG content of only 1.75 wt% is found to be 87.58 S/cm (shown in Fig. 8(2)), three orders of magnitude greater than that of pure PPy (0.52 S/cm). The conductivities of the final PPy/Ni/NanoG composites are dramatically increased compare to pure PPy.

3.6. Microwave absorbing properties

The electromagnetic parameters such as complex permittivity ($\varepsilon^* = \varepsilon' - j\varepsilon''$), complex permeability ($\mu^* = \mu' - j\mu''$), dielectric loss ($\tan\delta_e = \varepsilon''/\varepsilon'$) and magnetic loss ($\tan\delta_m = \mu''/\mu'$) of PPy, PPy/NanoG and PPy/Ni/NanoG were measured. Results are shown in Fig. 9. In the X band, the complex permittivities of all the materials are very high while their complex permeabilities are low. The complex permittivities and $\tan\delta_e$ of PPy/NanoG and PPy/Ni/NanoG are higher than those of PPy while the complex permeabilities and $\tan\delta_m$ of all the materials are almost equal.

Based on the measured data of the magnetic parameters, the microwave absorbing properties of the obtained samples can be calculated by the following equation [25,26]:

$$R = 20\log\left|\frac{Z_{in} - Z_0}{Z_{in} + Z_0}\right| \quad (8)$$

where R (dB) denotes to the reflection loss in decibel unit, Z_0 is the characteristic impedance of a vacuum, that is $Z_0 = (\mu_0\varepsilon_0)^{1/2} = 377\ \Omega$. Z_{in} is the input characteristic impedance at the absorbers/air interface, which can be expressed as:

$$Z_{in} = Z_0\left(\frac{\mu_r}{\varepsilon_r}\right)^{1/2}\tanh\left[j\left(\frac{2\pi ft}{c}\right)(\mu_r \times \varepsilon_r)^{1/2}\right] \quad (9)$$

where c is the velocity of light, t (2 mm) is the thickness of an absorber in millimeter, f is the frequency of microwave and μ_r and ε_r are the measured relative complex permeability and permittivity, respectively.

The calculated frequency dependence reflection losses of NanoG, Ni, PPy, Ni/NanoG and PPy/Ni/NanoG are shown in Fig. 10. The reflection loss of PPy is below −10 dB (90% absorption) at 9.2–12.4 GHz, the minimum loss value is −12.09 dB at 10.2 GHz. The bandwidth corresponding to the reflection loss below −10 dB

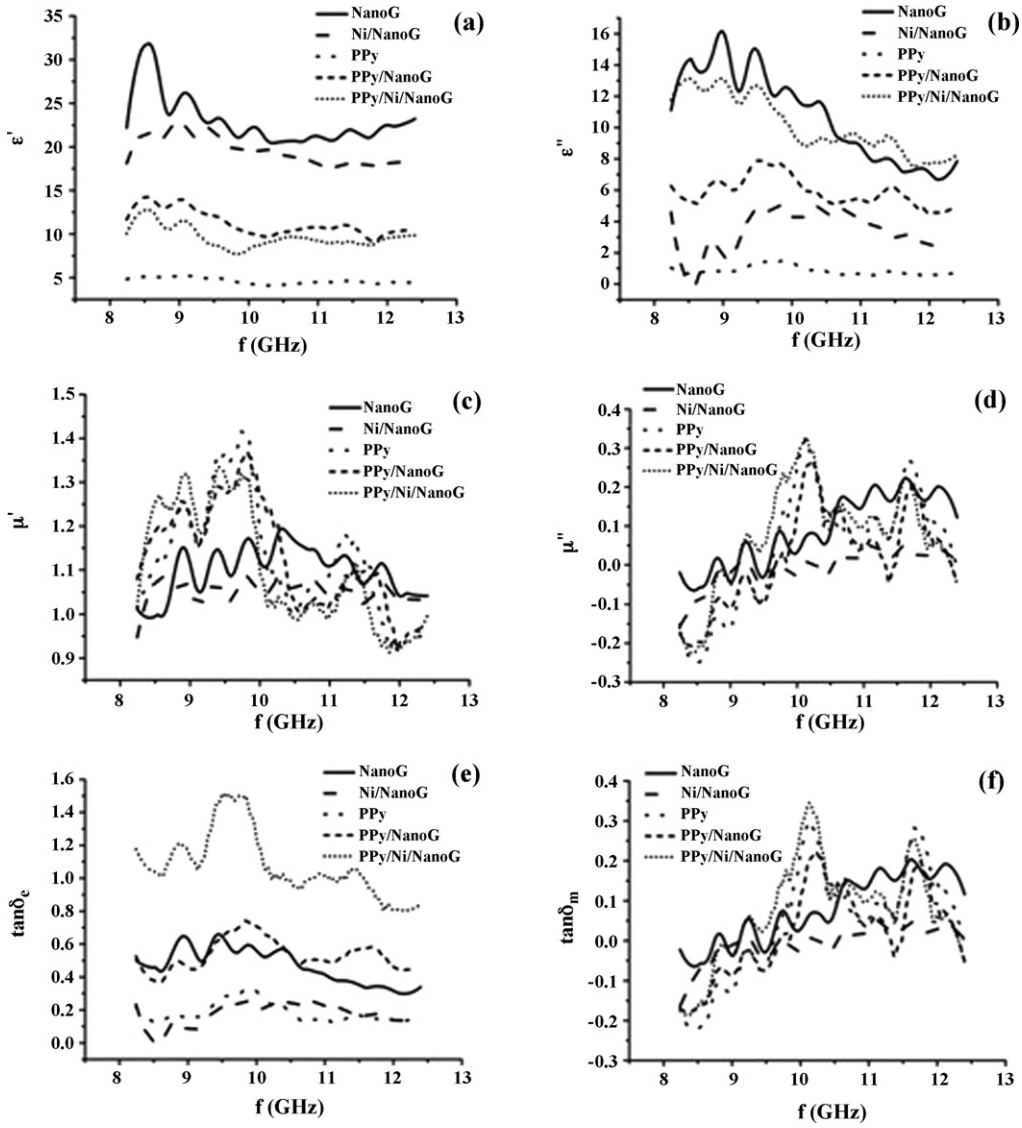

Fig. 9. Magnetic parameters of NanoG, Ni/NanoG, PPy, PPy/NanoG and PPy/Ni/NanoG.

is 3.2 GHz. To PPy/Ni/NanoG, the reflection loss of it is below −19 dB at 8.2–12.4 GHz and the minimum loss value is −23.46 dB at 9.88 GHz. The bandwidth corresponding to the reflection loss below −15 dB is 4.2 GHz. To PPy/NanoG, the reflection loss of it is below −10 dB at 8.2–12.4 GHz and the minimum loss value is −13.44 dB at 10.28 GHz. The bandwidth corresponding to the reflection loss below −10 dB is 4.2 GHz. The microwave absorbing properties of PPy/Ni/NanoG and PPy/NanoG are superior to those of PPy and can be used as good microwave absorbing materials.

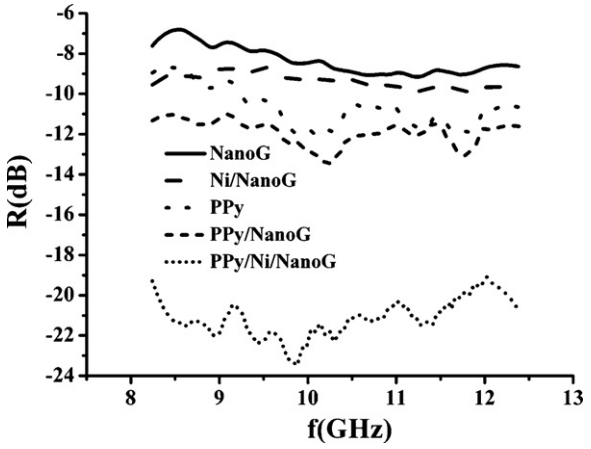

Fig. 10. Reflection losses of NanoG, Ni/NanoG, PPy, PPy/NanoG and PPy/Ni/NanoG.

4. Conclusions

In this paper, PPy/NanoG and PPy/Ni/NanoG were fabricated via in situ polymerization of pyrrole in the presence of NanoG and Ni/NanoG. The morphologies and nanostructures of NanoG, Ni/NanoG, PPy/NanoG and PPy/Ni/NanoG were characterized by SEM, EDS, FTIR and XRD respectively. Results show that NanoG has a great aspect ratio (300–500) and can be chemically coated by Ni. By in situ polymerization, most of NanoG and Ni/NanoG nanoparticles can be encapsulated by PPy. The thermogravimetric analysis suggests that with the introduction of nano-Ni and NanoG, the composites exhibit a better thermal stability than pure PPy. According to the four-point-probe test, the conductivities of the ultimate PPy/NanoG and PPy/Ni/NanoG composites are dramatically increased compared to pure PPy. Measurements of the reflection loss (R) show that the reflection loss of PPy/Ni/NanoG

is below −19 dB at 8.2–12.4 GHz and the minimum loss value is −23.46 dB at 9.88 GHz. The bandwidth corresponding to the reflection loss below −15 dB is 4.2 GHz. To PPy/NanoG, the reflection loss of it is below −10 dB at the X band and the minimum loss value is −13.44 dB at 10.28 GHz. The microwave absorbing properties of PPy/Ni/NanoG and PPy/NanoG are superior to those of PPy.

Acknowledgements

The authors would like to thank Professor Zhou and his student Doctor Qing from Department of Materials Science and Engineering, Northwestern Polytechnical University for their help in testing the electromagnetic parameters.

References

[1] S.H. Hosseini, S.H. Mohseni, A. Asadnia, H. Kerdari, J. Alloys Compd. 14 (2011) 4682–4687.
[2] J.H. Kim, S.S. Kim, J. Alloys Compd. 12 (2011) 4399–4403.
[3] W.C. Zhou, X.J. Hu, X.X. Bai, S.Y. Zhou, C.H. Sun, J. Yan, Appl. Mater. Interfaces 3 (2011) 3839–3845.
[4] G.B. Sun, B.X. Dong, M.H. Cao, B.Q. Wei, C.W. Hu, Chem. Mater. 23 (2011) 1587–1593.
[5] R.M. Khafagy, J. Alloys Compd. 41 (2011) 9849–9857.
[6] A.A. Farghali, M. Moussa, M.H. Khedr, J. Alloys Compd. 1 (2010) 98–103.
[7] X.F. Lu, W.J. Zhang, C. Wang, T.C. Wen, Y. Wei, Prog. Polym. Sci. 36 (2011) 671–712.
[8] Y.M. Bai, P. Qiu, Z.L. Wen, S.C. Han, J. Alloys Compd. 1 (2010) 1–4.
[9] H. Zhang, X. Zhong, J.J. Xu, H.Y. Chen, Langmuir 24 (2008) 13748–13752.
[10] Y.B. Li, G. Chen, Q.H. Li, G.Z. Qiu, X.H. Liu, J. Alloys Compd. 10 (2011) 4104–4107.
[11] H.Q. Chen, W. Wang, G.L. Li, C. Li, Y. Zhang, Synth. Met. 17–18 (2011) 1921–1927.
[12] Y. Yuan, S.G. Zhou, L. Zhuang, J. Power Sources 11 (2010) 3490–3493.
[13] B. Abraham, C.S. Rachel, B.T. Anna, Electrochim. Acta 22 (2011) 7651–7658.
[14] K. Ketpang, J.S. Park, Synth. Met. 15–16 (2010) 1603–1608.
[15] L.C. Li, C. Xiang, X.X. Liang, B. Hao, Synth. Met. 1–2 (2010) 28–34.
[16] Y.B. Li, G. Chen, Q.H. Li, G.Z. Qiu, X.H. Liu, J. Alloys Compd. 509 (2011) 4104–4107.
[17] Q.L. Li, C.R. Zhang, J.Q. Li, J. Alloys Compd. 509 (2011) 1953–1957.
[18] Q.W. Tang, J.H. Wu, H. Sun, S.J. Fang, J. Alloys Compd. 1–2 (2009) 429–433.
[19] W.F. Zhao, H.Q. Wang, H.T. Tang, G.H. Chen, Polymer 26 (2006) 8401–8405.
[20] T.S. Wang, G.H. Chen, C.L. Wu, D.J. Wu, Prog. Org. Coat. 2 (2007) 101–105.
[21] H. Fouad, R. Elleithy, J. Mech. Behav. Biomed. 7 (2011) 1376–1383.
[22] J.H. Li, H.F. Da, Q. Liu, S.S. Liu, Mater. Lett. 29–30 (2006) 3927–3930.
[23] S.C. Chanda, A. Manna, V. Vijayan, K. Pranaba, M. Nayak, H. Ashok, N. Acharya, Mater. Lett. 28 (2007) 5059–5062.
[24] A. Kambolis, H. Matralis, A. Trovarelli, C. Papadopoulou, Appl. Catal. A: Gen. 1–2 (2010) 16–26.
[25] V. Sunny, P. Kurian, P. Mohanan, P.A. Joy, M.R. Anantharaman, J. Alloys Compd. 1 (2010) 297–303.
[26] A. Maqsood, K. Khan, J. Alloys Compd. 7 (2011) 3393–3397.